Resolution of coherent and incoherent imaging systems reconsidered - Classical criteria and a statistical alternative

Sandra Van Aert and Dirk Van Dyck

University of Antwerp, Department of Physics, Groenenborgerlaan 171, 2020 Antwerp, Belgium

sandra.vanaert@ua.ac.be

Arnold J. den Dekker

Delft University of Technology, Delft Center for Systems and Control, Mekelweg 2, 2628 CD Delft, The Netherlands

Abstract: The resolution of coherent and incoherent imaging systems is usually evaluated in terms of classical resolution criteria, such as Rayleigh's. Based on these criteria, incoherent imaging is generally concluded to be 'better' than coherent imaging. However, this paper reveals some misconceptions in the application of the classical criteria, which may lead to wrong conclusions. Furthermore, it is shown that classical resolution criteria are no longer appropriate if images are interpreted quantitatively instead of qualitatively. Then one needs an alternative criterion to compare coherent and incoherent imaging systems objectively. Such a criterion, which relates resolution to statistical measurement precision, is proposed in this paper. It is applied in the field of electron microscopy, where the question whether coherent high resolution transmission electron microscopy (HRTEM) or incoherent annular dark field scanning transmission electron microscopy (ADF STEM) is preferable has been an issue of considerable debate.

© 2006 Optical Society of America

References and links

1. L. Rayleigh, "Wave theory of light," in *Scientific papers by Lord Rayleigh, John William Strutt*, (Cambridge University Press, Cambridge, 1902), Vol. 3, pp. 47-189.
2. J. W. Goodman, *Introduction to fourier optics* (McGraw-Hill, San Francisco, 1968).
3. A. J. den Dekker and A. van den Bos, "Resolution: A survey," J. Opt. Soc. Am. A **14,** 547-557 (1997).
4. V. Ronchi, "Resolving power of calculated and detected images," J. Opt. Soc. Am. **51,** 458-460 (1961).
5. L. Rayleigh, "On the theory of optical images, with special reference to the microscope," in *Scientific papers by Lord Rayleigh, John William Strutt*, (Cambridge University Press, Cambridge, 1903), Vol. 4, pp. 235-260.
6. J. C. H. Spence, *High-resolution electron microscopy, 3rd edition* (Oxford University Press, New York, 2003).
7. S. J. Pennycook and Y. Yan, "Z-contrast imaging in the scanning transmission electron microscope," in *Progress in transmission electron microscopy 1 - Concepts and techniques*, X.-F. Zhang and Z. Zhang, eds. (Springer-Verlag, Berlin, 2001), pp. 81-111.
8. P. D. Nellist and S. J. Pennycook, "Accurate structure determination from image reconstruction in ADF STEM," J. Microsc. **190,** 159-170 (1998).
9. D. Van Dyck and M. Op de Beeck, "A simple intuitive theory for electron diffraction," Ultramicroscopy **64,** 99-107 (1996).

10. S. Van Aert, A. J. den Dekker, A. van den Bos, and D. Van Dyck, "Statistical experimental design for quantitative atomic resolution transmission electron microscopy," in *Advances in Imaging and Electron Physics*, P. W. Hawkes, ed. (Academic Press, San Diego, 2004), Vol. 130, pp. 1-164.

11. A. J. den Dekker, S. Van Aert, D. Van Dyck, A. van den Bos, and P. Geuens, "Does a monochromator improve the precision in quantitative HRTEM?," Ultramicroscopy **89,** 275-290 (2001).

12. S. Van Aert, A. J. den Dekker, D. Van Dyck, and A. van den Bos, "Optimal experimental design of STEM measurement of atom column positions," Ultramicroscopy **90,** 273-289 (2002).

13. S. J. Pennycook, B. Rafferty, and P. D. Nellist, "Z-contrast imaging in an aberration-corrected scanning transmission electron microscope," Microsc. Microanal. **6,** 343-352 (2000).

14. O. Scherzer, "The theoretical resolution limit of the electron microscope," J. Appl. Phys. **20,** 20-28 (1949).

15. L. J. van Vliet, F. R. Boddeke, D. Sudar, and I. T. Young, "Image detectors for digital image microscopy," in *Digital image analysis of microbes; Imaging, morphometry, fluorometry and motility techniques and applications, modern microbiological methods*, M. H. F. Wilkinson and F. Schut, eds. (John Wiley and Sons, Chichester (UK), 1998), pp. 37-64.

16. A. van den Bos and A. J. den Dekker, "Resolution reconsidered - Conventional approaches and an alternative," in *Advances in Imaging and Electron Physics*, P. W. Hawkes, ed. (Academic Press, San Diego, 2001), Vol. 117, pp. 241-360.

17. A. J. den Dekker, S. Van Aert, A. van den Bos, and D. Van Dyck, "Maximum likelihood estimation of structure parameters from high resolution electron microscopy images. Part I: A theoretical framework," Ultramicroscopy **104,** 83-106 (2005).

1. Introduction

The question whether coherent or incoherent imaging is preferable in terms of resolution has given rise to many discussions. Usually this comparison is based on classical resolution criteria such as the well-known Rayleigh resolution criterion [1]. From this point of view, incoherent imaging is often concluded to be 'better' than coherent imaging, given that the same imaging system is used in both cases [2]. However, it will be shown in this paper that there are some misconceptions in the application of these classical criteria. The conclusion may be different if these criteria are applied properly, or preferably, if an alternative, more meaningful performance criterion is used.

Resolution is interpreted in many ways since it is not unambiguously defined. Therefore, several resolution criteria, including Rayleigh's, have been proposed in the past. These criteria may be defined using, for example, decision theory (considering resolution as a classification task), information theory or singularity theory. An overview of existing criteria may be found in [3]. The alternative criterion used in this paper is related to statistical measurement precision and will be used to evaluate coherent and incoherent imaging systems.

Coherent imaging is characterized by a fixed phase relationship between rays emerging from different parts of the object under study. Therefore, it is linear in complex amplitude. Such fixed phase relationships do not exist for incoherent imaging, which is linear in intensity. Using these linearity properties and knowledge of the point spread function, one can model, i.e., calculate, the image intensity distribution of two point sources for both types of imaging. Classical resolution criteria concern such *calculated* images [4]. However, calculated images have no practical meaning. In experimental physics, one is faced with *detected* images instead [4]. Therefore, practically relevant resolution criteria should concern detected images. Due to the inherent presence of noise, detected images will never be exactly describable by the chosen two-component model. If they were, fitting the model to the observations would result in an infinitely precise reconstruction of the locations of the components and there would be no limit to resolution. For detected images, model fitting never results in a perfect reconstruction. Resolution is then related to the limited statistical precision with which the component locations can be estimated. It will be shown that the attainable precision can be adequately quantified, making use of the physics behind the image formation process. Furthermore, it can be used as a more meaningful criterion to fairly compare the resolution of coherent and incoherent imaging systems.

2. Classical resolution criteria

Classical resolution criteria are based on calculated images. Generally, the model of a shift-invariant linear system can be expressed in terms of the point spread function. The image of two point objects which are illuminated coherently can be modelled as:

$$
\begin{aligned}
I(\mathbf{r}) &= |\delta(\mathbf{r}-\boldsymbol{\beta}_1)*t(\mathbf{r}-\boldsymbol{\beta}_1)+ \\
&\quad \exp(i\phi)\,\delta(\mathbf{r}-\boldsymbol{\beta}_2)*t(\mathbf{r}-\boldsymbol{\beta}_2)|^2 \\
&= |t(\mathbf{r}-\boldsymbol{\beta}_1)+\exp(i\phi)\,t(\mathbf{r}-\boldsymbol{\beta}_2)|^2
\end{aligned}
\tag{1}
$$

with $t(\mathbf{r})$ the coherent point spread function, $\delta(\mathbf{r})$ the Dirac delta function representing the scattering distribution of a point object, $\mathbf{r}=(x,y)$ a two-dimensional vector in the image plane, $\boldsymbol{\beta}_1$ and $\boldsymbol{\beta}_2$ the positions of the components, ϕ the relative phase between the two components, and $*$ the convolution operator. Using the same imaging system in the incoherent mode, the model becomes:

$$
\begin{aligned}
I(\mathbf{r}) &= |\delta(\mathbf{r}-\boldsymbol{\beta}_1)*t(\mathbf{r}-\boldsymbol{\beta}_1)|^2+ \\
&\quad |\exp(i\phi)\,\delta(\mathbf{r}-\boldsymbol{\beta}_2)*t(\mathbf{r}-\boldsymbol{\beta}_2)|^2 \\
&= |t(\mathbf{r}-\boldsymbol{\beta}_1)|^2+|t(\mathbf{r}-\boldsymbol{\beta}_2)|^2.
\end{aligned}
\tag{2}
$$

The incoherent point spread function is the squared modulus of the coherent point spread function, i.e., $|t(\mathbf{r})|^2$.

The most famous resolution criterion is that of Rayleigh [1]. It is based on presumed limitations to the resolving capabilities of the human visual system and originally states that two incoherent point sources of equal brightness are just resolved if the central maximum of the point spread function generated by one point source coincides with the first zero of the point spread function generated by the second. This criterion can be generalized to include point spread functions that have no zero in the neighborhood of their central maximum by taking the resolution limit as the distance for which the intensity at the central dip in the composite image is 81% of that at the maxima on either side. This corresponds to a central dip of 19% of the maximum intensity. After the introduction of this criterion, Rayleigh [5] and others [2] investigated the question whether two point sources, separated by the Rayleigh distance for incoherent point sources, would be easier or harder to resolve with coherent illumination than with incoherent illumination. Therefore, models as in Eq. (1) and (2) can be used and it is found that the answer depends on the *phase distribution* associated with these sources. When the sources are in quadrature ($\phi=\pi/2$), the image intensity distribution is identical to that resulting from incoherent point sources. When the sources are in phase ($\phi=0$), the dip in the image intensity distribution is absent and therefore the points are not as well resolved as for incoherent illumination. Finally, when the two point sources are in phase opposition ($\phi=\pi$), the dip is greater than 19%, and the two point sources are resolved better with coherent illumination than with incoherent illumination.

Another criterion is the so-called *diffraction limit to resolution*. This corresponds to the cutoff frequency of the transfer function being the frequency beyond which the transfer function of the system is zero. Since the transfer function and the point spread function are Fourier pairs, the cutoff frequency and the Rayleigh limit are closely related. The incoherent transfer function of a diffraction-limited system extends to a frequency that is twice the cutoff frequency of the coherent transfer function [2]. It is tempting, therefore, to conclude that incoherent imaging is better than coherent imaging. As emphasized by Goodman [2], this conclusion is in general not valid since the cutoff frequencies in the two cases are not directly comparable. The coherent cutoff determines the maximum frequency of the image amplitude, while the incoherent cutoff refers to frequency components of the image intensity.

Consider now a practical example from the field of electron microscopy where there is a continuing discussion whether coherent HRTEM or incoherent ADF STEM is preferable. In HRTEM [6], the material under study is illuminated by a coherent, nearly plane wave electron source. The electrons are transmitted through the material and interact with it. Next, a magnified image of the scattered wave is formed. In ADF STEM [7], a probe scans in a raster over the material. At each probe position, an annular detector placed in the back focal plane beyond the material collects a fraction of the total scattering, more specifically, all electrons transmitted through the material but scattered to relatively high angles. From the so-called principle of reciprocity [6], it follows that the ADF detector is equivalent to using a large incoherent illuminating source in HRTEM. The arguments which are generally used to prefer ADF STEM over HRTEM are based on the apparent better resolution of incoherent illumination compared to coherent illumination if identical components are considered for which $\phi = 0$ [7, 8]. However, this conclusion is only justifiable if the model for coherent HRTEM and incoherent ADF STEM imaging is of the same form as in Eq. (1) and (2), respectively. It is therefore important to take these models into consideration. In case of HRTEM, for which the material is usually oriented along a main crystal zone axis (i.e., parallel with the atom columns), the model can be written as follows [9, 10, 11]:

$$I(\mathbf{r}) = \left| 1 + \sum_{n=1}^{n_c} a_n \varphi_{1s,n}(\mathbf{r} - \boldsymbol{\beta}_n) * t(\mathbf{r} - \boldsymbol{\beta}_n) \right|^2, \quad (3)$$

where the atom column approximation is made. In Eq. (3), n_c represents the total number of atom columns being imaged, the function $\varphi_{1s,n}(\mathbf{r} - \boldsymbol{\beta}_n)$ is the lowest energy bound state of the nth atom column located at position $\boldsymbol{\beta}_n$, $t(\mathbf{r})$ is the point spread function of the electron microscope, a_n is a complex coefficient depending among other parameters on the thickness z of the material. From the comparison of Eq. (3) with Eq. (1), it may be concluded that the Dirac delta function is now replaced with $\varphi_{1s,n}(\mathbf{r})$, which is a function of finite size. This expresses the fact that atoms may not be considered to be point scatterers. The most important difference is the presence of the term '1' in Eq. (3), which is absent in Eq. (1). It represents an unscattered wave, which in classical terms means that part of the incident electrons will not scatter in the material, but may interfere with the scattered electrons. Let us now consider ADF STEM assuming the same material being imaged using a microscope with the same lens characteristics as in HRTEM. If the atom column approximation is made, the model is given by [10, 12, 13]:

$$I(\mathbf{r}) = \sum_{n=1}^{n_c} A_n |\varphi_{1s,n}(\mathbf{r} - \boldsymbol{\beta}_n) * t(\mathbf{r} - \boldsymbol{\beta}_n)|^2 \quad (4)$$

with A_n a factor depending among other parameters on the thickness z and on the detector geometry. From the comparison of Eq. (4) with Eq. (2), it may be concluded that these models are equivalent apart from the replacement of the Dirac delta function with a function of finite size. Note that in the derivation of Eq. (4), only elastic scattering has been considered and not thermal diffuse, inelastic scattering. The incoherent characteristics of the model are therefore not caused by incoherent scattering events but are purely created by the detector geometry [13].

To study whether the presence of the term '1' in Eq. (3) affects the conclusion on which instrument is preferable in the sense of Rayleigh, HRTEM and ADF STEM images of two neighboring, identical Si[110] atom columns have been simulated as a function of thickness. The distance between the columns is equal to 1.36 Å. For HRTEM as well as for ADF STEM, the so-called spherical aberration constant of the microscope and the electron wavelength are chosen equal to 0.2 mm and 0.02 Å, respectively. These settings mainly determine the optimal width of the microscope's point spread function with the other settings, like defocus and objective aperture radius, chosen in accordance with the so-called Scherzer conditions for coherent
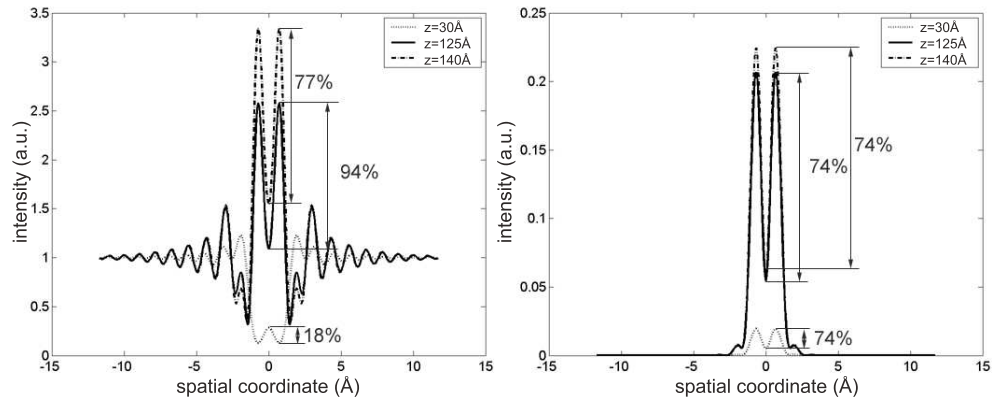
Fig. 1. Cross sections of HRTEM and ADF STEM intensity distributions for different thicknesses. The height of the central dip relative to the maximum or minimum intensity above or below the background is indicated.

and incoherent imaging, respectively [6, 7, 14]. In Fig. 1, cross sections of the HRTEM and ADF STEM intensity distributions are shown for different thicknesses. Furthermore, the height of the central dip relative to the maximum or minimum intensity above or below the background is indicated. If this value is equal to 19% or more, the columns are resolved, if it is less than 19%, the columns are not resolved. This criterion is the usual extension of Rayleigh's in case of a background [14]. From Fig. 1, it can be seen that the significant value varies as a function of thickness for HRTEM whereas it is a constant for ADF STEM. From the comparison of the corresponding values, it follows that for certain thicknesses, the columns are resolved better with HRTEM than with ADF STEM. This result appears even in the absence of a phase difference between the two columns and is due to the presence of the term '1' in Eq. (3). Note that for HRTEM a phase difference will exist between two neighboring atom columns if they consist of different elements or if they have a different thickness. This example illustrates that the optimal choice between coherent or incoherent imaging systems in the sense of Rayleigh does not only depend on the phase distribution associated with the object but also on the structure of the models describing the image intensity distribution.

3. Attainable precision

Classical resolution criteria are concerned with calculated images, that is, noise-free images exactly describable by a known parameterized model. However, these criteria disregard the possibility of using this a priori knowledge about the image intensity distribution to extract numerical results from the observations by model fitting using parameter estimation methods. Since Rayleigh's days, visual inspection has been supplemented with intensity measuring instrumentation and digital computing facilities, which make model fitting manageable. If observations would be exactly describable by a physics based model, the resulting fit would be perfect and there would be no limit to resolution. However, despite continuous technical progress, which provides us with detectors which are able to count single photons, images exactly describable by a model do not exist. This is due to the inherent presence of noise in the images resulting, for example, from the intrinsic quantum nature of light. Indeed, photon production by any light or electron source is a statistical process governed by the laws of quantum physics. The source emits photons at random time intervals. The number of photons in a fixed observation interval will result in a number that obeys Poisson statistics [15]. It is such statistical fluctuations of the

observations which prevent parameter estimation methods to result in a perfect fit. Resolution is then related to the statistical precision with which the component locations can be estimated.

Given the physical model behind the image formation process and knowledge about the statistics of the observations, the *attainable* precision can be adequately quantified in the form of the so-called *Cramér-Rao lower bound* (CRLB). This is a lower bound on the variance of any unbiased estimator of a parameter. The meaning of this lower bound is as follows. One can use different parameter estimation methods in order to estimate unknown parameters, such as the least squares or the maximum likelihood (ML) estimator. The precision of an estimator is represented by the variance or by its square root, the standard deviation. Generally, different estimators will have different precisions. It can be shown, however, that the variance of unbiased estimators will never be lower than the CRLB. Fortunately, there exists a class of estimators (including the ML estimator) that achieves this bound at least asymptotically, that is, for the number of observations going to infinity. A summary of the different steps involved to compute the CRLB is given below. A more detailed description may be found in [16, 17].

First, an expression for the joint probability density function of the observations and its dependence on the unknown parameters should be established. For independent, Poisson distributed observations, the probability $P(\omega;\theta)$ that a set of observations $w = (w_1...w_M)^T$ is equal to $\omega = (\omega_1...\omega_M)^T$ is given by:

$$P(\omega;\theta) = \prod_{m=1}^{M} \frac{\lambda_m^{\omega_m}}{\omega_m!} \exp(-\lambda_m) \tag{5}$$

with λ_m the expectation of the observation w_m. In Eq. (5), it is supposed that these expectations are described by an expectation model, that is, a physical model, which contains the parameters θ to be estimated, such as the x- and y- coordinates of the positions $\boldsymbol{\beta}_1$ and $\boldsymbol{\beta}_2$ of components or atom columns. As follows from section 2, such a model exists for coherent and incoherent imaging systems. It is given by:

$$\lambda_m = \frac{N}{C} \int_{S_m} I(\mathbf{r})\, d\mathbf{r} \approx \frac{N}{C} I(\mathbf{r_m}) S_m \tag{6}$$

with $I(\mathbf{r})$ given by Eqs. (1)-(4), $\mathbf{r}_m, m = 1,...,M$ the measurement points, $S_m, m = 1,...,M$ the area of these measurement points, N the total number of detected counts in an image, and C a normalization factor so that the integral of the function $I(\mathbf{r})/C$ is equal to one.

Next, the so-called *Fisher information matrix F* with respect to the elements of the $T \times 1$ parameter vector $\theta = (\theta_1...\theta_T)^T$ is introduced. It is defined as the $T \times T$ matrix

$$F = -E\left[\frac{\partial^2 \ln P(w;\theta)}{\partial\theta\, \partial\theta^T}\right], \tag{7}$$

where $P(\omega;\theta)$ is the joint probability density function of the observations $w = (w_1...w_M)^T$. The expression between square brackets represents the Hessian matrix of $\ln P$, for which the (r,s)th element is defined by $\partial^2 \ln P(\omega;\theta)/\partial\theta_r\partial\theta_s$. For independent, Poisson distributed observations, where $P(\omega;\theta)$ is given by Eq. (5), it follows that the (r,s)th element of F is equal to:

$$F_{rs} = \sum_{m=1}^{M} \frac{1}{\lambda_m} \frac{\partial\lambda_m}{\partial\theta_r} \frac{\partial\lambda_m}{\partial\theta_s}. \tag{8}$$

Thus, it can be used to obtain an expression for the Fisher information matrix with respect to the x- and y-coordinates of the positions $\boldsymbol{\beta}_1$ and $\boldsymbol{\beta}_2$. Assuming that these position coordinates are the only parameters to be estimated, the parameter vector θ is given by $\theta = (\beta_{x1}\ \beta_{x2}\ \beta_{y1}\ \beta_{y2})^T$.

An expression for the elements of the Fisher information matrix is found by substitution of the expectation model given by Eq. (6) and its derivatives with respect to the unknown parameters into Eq. (8):

$$F_{rs} = \frac{NS_m}{C} \sum_{m=1}^{M} \frac{1}{I(\mathbf{r}_m)} \frac{\partial I(\mathbf{r}_m)}{\partial \theta_r} \frac{\partial I(\mathbf{r}_m)}{\partial \theta_s} \tag{9}$$

with $I(\mathbf{r}_m)$ the image model given by Eqs. (1)-(4). Recall that the model $I(\mathbf{r}_m)$ depends, among other things, on the relative phase between two points and on the spherical aberration constant and defocus determining the point spread function. Furthermore, the number of detected counts N depends on the brightness of the source, the source diameter, and the recording time. Therefore, the elements F_{rs}, given by Eq. (9), will depend on all these microscope settings as well. Explicit numbers for these elements are obtained by substituting values of a given set of microscope settings and position coordinates of the components or atom columns into Eq. (9).

It can be shown that the covariance matrix $cov(\widehat{\theta})$ of any unbiased estimator $\widehat{\theta}$ of θ satisfies:

$$cov(\widehat{\theta}) \geq F^{-1} \tag{10}$$

This inequality expresses that the difference of the matrices $cov(\widehat{\theta})$ and F^{-1} is positive semidefinite. Since the diagonal elements of $cov(\widehat{\theta})$ represent the variances of $\widehat{\theta}_1, ..., \widehat{\theta}_T$ and since the diagonal elements of a positive semidefinite matrix are nonnegative, these variances are larger than or equal to the corresponding diagonal elements of F^{-1}:

$$var(\widehat{\theta}_r) \geq \left[F^{-1}\right]_{rr}, \tag{11}$$

where $r = 1, ..., T$ and $[F^{-1}]_{rr}$ is the (r,r)th element of the inverse of the Fisher information matrix. In this sense, F^{-1} represents a lower bound to the variances of all unbiased $\widehat{\theta}$. The matrix F^{-1} is called the CRLB on the variance of $\widehat{\theta}$.

Finally, the CRLB can be extended to include unbiased estimators of vectors of functions of the parameters instead of the parameters proper. Let $\gamma(\theta) = (\gamma_1(\theta)...\gamma_C(\theta))^T$ be such a vector and let $\widehat{\gamma}$ be an unbiased estimator of $\gamma(\theta)$. Then, it can be shown that

$$cov(\widehat{\gamma}) \geq \frac{\partial \gamma}{\partial \theta^T} F^{-1} \frac{\partial \gamma^T}{\partial \theta} \tag{12}$$

where $\partial \gamma / \partial \theta^T$ is the $C \times T$ Jacobian matrix defined by its (r,s)th element $\partial \gamma_r / \partial \theta_s$. The right-hand member of this inequality is the CRLB on the variance of $\widehat{\gamma}$. It can be used to compute the scalar valued CRLB on the variance of unbiased estimators of the distance $\delta = \sqrt{(\boldsymbol{\beta}_{1x} - \boldsymbol{\beta}_{2x})^2 + (\boldsymbol{\beta}_{1y} - \boldsymbol{\beta}_{2y})^2}$ between two point source objects from the CRLB on the variance of estimators of the x- and y-coordinates of the positions $\boldsymbol{\beta}_1$ and $\boldsymbol{\beta}_2$. Equation (12) is then equal to:

$$var\left(\widehat{\delta}\right) \geq \frac{\partial \delta}{\partial \theta^T} F^{-1} \frac{\partial \delta^T}{\partial \theta} \tag{13}$$

with $\theta = (\beta_{x1} \ \beta_{x2} \ \beta_{y1} \ \beta_{y2})^T$, the elements of F given by Eq. (9), and

$$\frac{\partial \delta}{\partial \theta^T} = \frac{1}{\delta} \left(\ \beta_{x1} - \beta_{x2} \quad \beta_{x2} - \beta_{x1} \quad \beta_{y1} - \beta_{y2} \quad \beta_{y2} - \beta_{y1} \ \right). \tag{14}$$

It follows from Eq. (9) that the right-hand member of Eq. (13) is inversely proportional to the number of detected counts N. This means that the distance δ can be estimated more precisely if the dose increases. The final expression defining the CRLB on the variance of unbiased
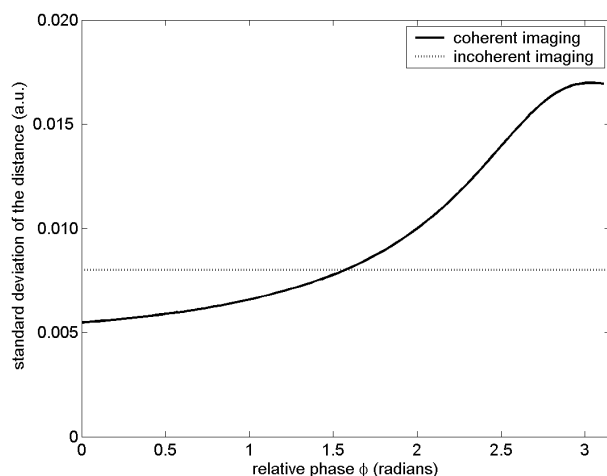
Fig. 2. Lower bound on the standard deviation of the distance for two point sources separated by the Rayleigh distance as a function of the relative phase ϕ.

estimators of the distance δ, given by the right-hand member of Eq. (13), can be considered as an alternative, nowadays more meaningful, criterion of resolution.

Following the procedure described in the previous paragraph, the lower bound on the standard deviation of the distance, that is, the square root of the CRLB, has been computed as a function of the relative phase ϕ for two point sources separated by the Rayleigh distance (for incoherent point sources) and assuming the function $t(\mathbf{r})$ in Eqs. (1) and (2) to be the square root of the well-known Airy disk. For both imaging modes, the total number of photons to form the image has been assumed to be the same. Furthermore, throughout this paper, the pixel size has been chosen in the region where any further decrease only slightly improves the precision [10]. The results are shown in Fig. 2. This figure can be used to find out if the distance could be estimated more or less precisely with coherent imaging than with incoherent imaging. It follows that the precision for coherent imaging is identical to that of incoherent imaging if the relative phase between the two point objects is equal to $\pi/2$. The reason for this is that the models given by Eqs. (1) and (2) are identical in this case. Furthermore, it follows that coherent imaging is preferable in terms of precision if the relative phase is less than $\pi/2$. If it is larger than $\pi/2$, incoherent imaging is preferable. This result is exactly the opposite of what is found in terms of Rayleigh resolution. It can be understood by carrying out simulation experiments and subsequent estimation of the position coordinates using the ML estimator. By analyzing these results it can be shown that the ML estimator attains the CRLB and that the bias is undetectably small at the distance considered. For relative phases less than $\pi/2$ the ML estimates of the position coordinates are stronger correlated than for relative phases larger than $\pi/2$. A stronger correlation of the position coordinates affects the precision of the distance in a favorable way.

Finally, the concept of resolution in terms of the CRLB is used to objectively compare coherent HRTEM and incoherent ADF STEM. In Fig. 3, the lower bound on the standard deviation of the distance between two Si[110] columns is shown as a function of the field of view for HRTEM and ADF STEM. This lower bound has been computed by substituting Eq. (9) into the square root of the right-hand member of Eq. (13). The image model in Eq. (9) is given by Eq. (3) and (4) for HRTEM and ADF STEM, respectively. A detailed description of these two models and an expression for the number of detected counts N are outside the scope of this
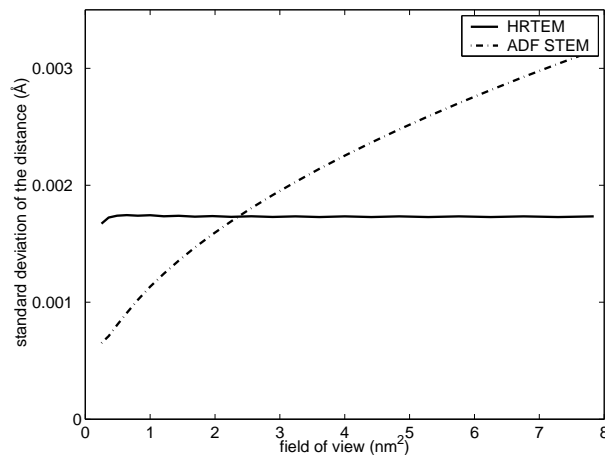
Fig. 3. Lower bound on the standard deviation of the distance between two Si[110] columns for HRTEM and ADF STEM as a function of the field of view. The recording time and pixel size are kept constant in this evaluation.

paper, but can be found in [11] and [12] for HRTEM and ADF STEM, respectively. The computation of the lower bound is done for a microscope with a spherical aberration constant and electron wavelength equal to 0.5 mm and 0.02 Å, respectively. The other microscope settings have been adjusted to their optimal values according to the principles of statistical experimental design. In brief, this means that those microscope settings correspond to the minimum of the CRLB. A comprehensive report of these principles can be found in [10, 11, 12]. In the computation of Fig. 3, the total recording time is kept constant presuming that specimen drift puts a practical constraint to the experiment. Since ADF STEM images are recorded by scanning a probe over the material, a larger field of view implies a larger scan speed and therefore less incident electrons per probe position. This has an unfavorable effect on the precision leading to an increase of the standard deviation for increasing field of view. It is related to the fact that the lower bound on the variance of the distance is inversely proportional to the number of detected counts N as mentioned before. From Fig. 3, it can be seen that for small field of views, that is, less than 2 nm^2 in this example, ADF STEM is preferable in terms of precision, otherwise HRTEM is preferable. It should be emphasized that these results cannot be explained using a Rayleigh-type criterion since such a criterion does not take account of, for example, the electron dose. Furthermore, using the CRLB it can be shown that if it is radiation sensitivity of the material rather than specimen drift which puts a constraint to the experiment, the incident electron dose per square Å has to be kept constant. In that case, HRTEM is usually preferred.

4. Conclusions

In conclusion, we proposed a quantitative resolution criterion that can be used to compare the performance of coherent and incoherent imaging systems. By expressing resolution in terms of the precision with which the distance between neighboring objects can be estimated, the proposed criterion reflects the purpose of quantitative experiments, that is, precise measurement of physical parameters. As such, it may replace Rayleigh-like classical resolution criteria that express the possibility to visually distinguish neighboring objects. Based on Rayleigh's resolution criterion, incoherent imaging is often found to be better than coherent imaging. However, this conclusion is only true if there is no phase difference between rays emerging from two neigh-

boring point sources. If there is a phase difference of π, coherent imaging is preferred. In terms of precision the conclusion is just the contrary. Moreover, we applied both Rayleigh's resolution criterion and the precision based alternative in the field of electron microscopy, comparing coherent HRTEM and incoherent ADF STEM. In terms of Rayleigh we found that depending on the material thickness, HRTEM may be preferable even in the absence of a phase difference between neighboring atom columns. In terms of precision we found that HRTEM is usually preferable, except for fields of view smaller than a few squared nanometers.

Acknowledgments